



1 *Manuscript – technical note*

2 **Analysis of oxygen isotopes of inorganic phosphate**
3 **($\delta^{18}\text{O}_p$) in freshwater: A detailed method description**

4 **Catharina Simone Nisbeth**¹, **Federica Tamburini**², **Jacob Kidmose**³, **Soren Jessen**¹ and **David**
5 **William O’Connell**^{4,*}

6 ¹ Department of Geosciences and Natural Resource Management (IGN), University of Copenhagen, Øster
7 Voldgade 10, 1350 Copenhagen K, Denmark

8 ² Institute of Agricultural Sciences, ETH Zurich, 8315 Lindau, Switzerland.

9 ³ Geological Survey of Denmark and Greenland (GEUS), Øster Voldgade 10, 1350 Copenhagen K, Denmark

10 ⁴ Department of Civil, Structural and Environmental Engineering, Trinity College Dublin, College Green,
11 Museum Building, Dublin 2, Ireland.

12
13 * Correspondence: connedw@tcd.ie (D.W.O.)

14 **Abstract:** The ability to identify the origin of phosphorus is essential to effectively mitigate
15 eutrophication of freshwater ecosystems. The oxygen isotope composition of orthophosphate ($\delta^{18}\text{O}_p$)
16 has been suggested to have a significant prospective as a tracer for P entering freshwater ecosystems.
17 The $\delta^{18}\text{O}_p$ tracing method is, however, still in its preliminary stages and has proven challenging to
18 implement for new practitioners. In order to achieve progress in developing the application of $\delta^{18}\text{O}_p$
19 signatures as a tracing tool, there is a need to eliminate the methodological challenges involved in
20 accurately determining $\delta^{18}\text{O}_p$. This technical note describes the various steps needed to concentrate
21 and isolate orthophosphate in freshwater samples into an adequately pure analyte (Ag_3PO_4), without
22 isotopic alteration during processing. The protocol compiles the disperse experiences from previous
23 studies, combined with our own experience.

24

25



26 1. Introduction

27 In freshwater ecosystems, phosphorus (P) is usually the primary limiting nutrient for growth of
28 macrophytes, algae and cyanobacteria. Increased P concentrations can therefore result in
29 eutrophication, anoxia and degradation of water quality in lakes, rivers and streams (Blake et al.,
30 2005; Hecky & Kilham, 1988; Wetzel, 2001). Phosphorus input to surface water aquatic ecosystems
31 originates from various sources including septic tanks, waste water treatment plants, agricultural
32 fertilizers, animal excreta and dissolved minerals (Heiberg et al., 2012; Marion et al., 1994; Quinton et
33 al., 2010; Sharpley et al., 2003). Thus, identifying the various potential phosphorus sources and their
34 relative contribution to the total phosphorus load is essential for restoration and improvement of
35 eutrophic aquatic ecosystems (Elsbury et al., 2009; McLaughlin, Kendall, et al., 2006).

36 Identification of the source and apportioning the contributions of phosphorus discharging to
37 surface water from various sources is not a trivial matter and requires an appropriate tracer, which
38 can accommodate this complexity (Jaisi et al., 2011). An ideal tracer is part of the phosphate molecule
39 without changing its properties.

40 Dissolved inorganic orthophosphate (referred to as P_i hereafter) is the primary form of P cycled
41 through ecosystems (Moorleghem et al., 2013). Hence, the stable oxygen isotope of inorganic
42 phosphate ($\delta^{18}O_p$, in which the subscript 'p' denotes 'phosphate') has been suggested as a significant
43 prospective tracer for P cycling in the environment (Blake et al., 1997, 2005; Colman, 2002; Jaisi &
44 Blake, 2014; McLaughlin et al., 2004). The $\delta^{18}O_p$ can be used as a tracer, since the P-O bond in P_i is
45 resistant to inorganic hydrolysis at temperatures and pH levels found in natural abiotic aquatic
46 ecosystems (Blake et al., 1997; Liang & Blake, 2007; Longinelli et al., 1976). Subsequently, the $\delta^{18}O_p$
47 value in abiotic aquatic ecosystems will reflect the isotopic signature of the P sources (Tamburini et
48 al., 2010; Zohar et al., 2010). Biological mediation in aquatic ecosystems can, however, alter the source
49 $\delta^{18}O_p$ signatures, through biological uptake and recycling. This will result in an isotopic equilibrium
50 between the stable oxygen isotopes in the ambient water ($\delta^{18}O_w$) and the P_i sources (Blake et al., 2005).
51 Consequently, the $\delta^{18}O_p$ value in abiotic aquatic ecosystems will only reflect the isotopic signature of
52 the P sources when the biological activity is relatively low compared to the input of P_i .

53 1.1. The $\delta^{18}O_p$ -method

54 Traditionally, the determination of $\delta^{18}O_p$ was established through fluorination (Crowson et al.,
55 1991; Longinelli, 1966) or bromination of a phosphate precipitate, which generally was in the form of
56 bismuth(III)-phosphate ($BiPO_4$) (Kolodny et al., 1983; Longinelli et al., 1976; Longinelli & Nuti, 1973b,
57 1973a; Shemesh et al., 1983, 1988). The $BiPO_4$ precipitate is a hygroscopic material that rehydrates
58 within 15 minutes after dehydration, hence significant preparation is required before isotopic
59 analysis. Recent methods use silver(I) phosphate (Ag_3PO_4) (Colman, 2002; Crowson et al., 1991;
60 Lécuyer, 2004; Tamburini et al., 2010) which is less hygroscopic, is stable, has low solubility, and
61 results in better O yield during quantitative conversion of the PO_4 -O to CO-O, and requires less
62 preparation time (Crowson et al., 1991; Firsching, 1961). Multivalent ions and silicates interfere with
63 Ag_3PO_4 precipitation, however low valence ions did not impact precipitation (i.e. NO_3^- , NH_4^+ and K^+)
64 (Firsching, 1961).

65 Accordingly, Ag_3PO_4 precipitation has become the most popular method for $\delta^{18}O_p$ in aqueous
66 and terrestrial environments due to improved extraction protocols enabling sufficient precipitation
67 of Ag_3PO_4 for analysis from low inorganic phosphorus concentration matrices (Elsbury et al., 2009;
68 Goldhammer et al., 2011; Granger et al., 2017; McLaughlin et al., 2004; Pistocchi et al., 2017; Tamburini
69 et al., 2010; Zohar et al., 2010). $\delta^{18}O_p$ can be analyzed by thermal conversion/elemental analyser
70 isotope ratio mass spectrometry (TC/EA-IRMS). The Ag_3PO_4 precipitation technique for TC/EA-IRMS
71 has many advantages over the traditional fluorination technique in that (i) small PO_4 quantities are
72 required for the analysis (yielding ~300-600 μg Ag_3PO_4); (ii) dangerous chemicals are avoided, such
73 as BrF_3 , F_2 or ClF_3 ; and (iii) measurements are automated (Vennemann et al., 2002).



74 1.2. *Approaching a uniform P_i extraction method via Ag₃PO₄ precipitation*

75 Several detailed protocols for the extraction of P_i via precipitation of Ag₃PO₄ from different
76 complex matrix solutions such as fresh and ocean waters and soil extractions exist (Colman, 2002;
77 Goldhammer et al., 2011; Gruau et al., 2005; McLaughlin et al., 2004; Tamburini et al., 2010, Zohar et
78 al., 2010). The major techniques for these protocols have been summarized by Paytan & McLaughlin
79 (2011) and Davies et al. (2014).

80 For water samples, the broadly common sequence of steps for Ag₃PO₄ precipitation is this: (i) P_i
81 is quantitatively removed from the sample through magnesium-induced co-precipitation (MagIC) by
82 brucite (Karl & Tien, 1992); (ii) redissolution of the brucite-pellet in an acid matrix, which resuspends
83 the P_i in solution; (iii) removal of other interfering sources of O, such as dissolved organic matter
84 (DOM), by using anion exchange resins and/or sequential precipitations; (iv) removal of potentially
85 interfering cations using a cation exchange resin; (v) precipitation of Ag₃PO₄. All steps are designed
86 to inhibit isotopic fractionation.

87 One of the major challenges with all the Ag₃PO₄ precipitation methods relates to the insufficient
88 removal of oxygen sources other than phosphate (Tamburini et al., 2010). Thus, the purification steps
89 are of great importance. Especially DOM is of concern as the high O content of DOM can significantly
90 interfere with the measured fractionation of δ¹⁸O_P and persists throughout all sequential steps of the
91 Ag₃PO₄ precipitation methods (McLaughlin, Paytan, et al., 2006).

92 There is a variety of approaches to address this problem, including *a*) adsorption of organic
93 compounds to phosphate-free activated carbon (Gruau et al., 2005) or to a resin such as DAX-8
94 (Colman, 2002; Joshi et al., 2018; Tamburini et al., 2010), *b*) repetition of the MagIC step with the
95 intention of further isolation of P_i from a matrix with potential contaminants (Colman, 2002;
96 Goldhammer et al., 2011), *c*) acidified pH-specific precipitations of fulvic and/or humic acids (Zohar
97 et al., 2010), *d*) sequential precipitation and re-crystallization scheme to efficiently scavenge P_i
98 (Tamburini et al., 2010), *e*) and a final washing of the Ag₃PO₄ precipitate with hydrogen peroxide to
99 eliminate residual organic matter by oxidation (Goldhammer et al., 2011; Tamburini et al., 2010;
100 Zohar et al., 2010).

101 Despite the several existing protocols and the review papers by Paytan & McLaughlin (2011)
102 and Davies et al. (2014) focusing on analysis of the δ¹⁸O_P of inorganic phosphate, and despite
103 numerous articles describing δ¹⁸O_P application in different aquatic environments, there exists
104 currently no collective or uniform protocol via precipitation of Ag₃PO₄ for freshwater matrices. This
105 is further despite the fact that the method can prove challenging to implement for new practitioners.
106 In addition, some of the common steps were originally developed and documented for other
107 conditions than they are now applied on. For example, the MagIC steps' quantitative P_i removal was
108 well documented, but for the matrix of oceanic seawater, which is relatively invariable compared to
109 freshwater matrices. Nevertheless, it has nearly directly been applied on freshwater samples. Hence,
110 to make the method as widely and practically applicable as possible, and to facilitate proper grounds
111 for a coherent future method development aiming at freshwater systems, there is a need for a detailed
112 method description for the Ag₃PO₄ precipitation method. The present technical note aims to address
113 the needs with (i) describing each step of the Ag₃PO₄ precipitation method in detail; (ii) explain the
114 historical background and reasoning behind each step; (iii) compile from the literature the (lacking)
115 documentation of individual steps; (iv) give practical advice and suggestions to tackle potential
116 challenges which may arise when applying the method, as it is, under different scenarios.

117 **2. Protocol for freshwater δ¹⁸O_P determination**

118 2.1. *Reading guide for the protocol*

119 The protocol (Sections 2.2, 2.3 and 2.4) is about concentration and isolation of P_i in freshwater
120 samples and result in an adequately pure solid silver phosphate crystal (Ag₃PO₄), without isotopic
121 alteration. The description of the subsequent TC/EA-IRMS analysis of the δ¹⁸O_P determination is not
122 included. For that, we refer to Tamburini et al. (2010) or Davies et al. (2014).



123 The protocol can be used when water sampling volumes are not restricted. In situations where
124 sampling is difficult and sample volumes limited, we refer to the method presented by Goldhammer
125 et al. (2011). If the goal is to determine $\delta^{18}\text{O}_p$ from a sediment sample, we refer to the P extraction
126 method presented by Tamburini et al. (2010).

127 The here presented protocol consists of three sections: Section 2.2 'Freshwater sampling', Section
128 2.3 'Quantitative P_i removal by the MagIC method', and Section 2.4 'Purification and silver phosphate
129 precipitation'. Each section is divided into main steps presented by roman numerals and each main
130 step is further subdivided into substeps indicated by letters from the Latin alphabet.

131 Three different remarks will be presented throughout the protocol:

132 *Note*Specific concerns to be aware of when performing one of the substeps.

133 *We experienced*Phenomena we have experienced that have not been presented in earlier
134 method descriptions.

135 *Method disagreement*Draws attention to steps where there are inconsistencies between already
136 published $\delta^{18}\text{O}_p$ methods.

137

138 The protocol compiles the diverse experiences from previous studies, combined with our own
139 experience. Description of the preparation of all used chemicals and reagents are provided in
140 Appendix A.

141 2.2. Freshwater sampling

142 The amount of water to be sampled depends on the P_i concentration of the sampled water itself.
143 It is recommended to sample a minimum of 20 μmol s of P. This will provide enough P to allow some
144 P losses from one step to the next and thus an easier handling of the protocol. This can lead to required
145 water volumes of 10 to 50 L for P_i concentrations of 2 and 0.4 μM , respectively (McLaughlin et al.,
146 2004; Tamburini et al., 2010).

147 It is important to take the necessary precaution in relation to the type of water being sampled.
148 This is especially true when sampling anoxic and Fe^{2+} -rich water where P_i co-precipitation with Fe(III)-
149 (hydr)oxides (henceforth collectively referred to as Fe-oxides), forming upon contact which
150 atmospheric O_2 could immediately occur (Senn et al., 2015). Thus, different sampling approaches are
151 needed when working with either oxic or anoxic samples:

152 Step I. Freshwater sampling

153 *a)* Prior to sampling, acid-wash, rinse with deionized distilled water ($\text{DD-H}_2\text{O}$), and air dry a
154 polyethylene collection container. If planning to sample anoxic and Fe^{2+} -rich water, additionally
155 flush the container with N_2 gas and seal the container. *b)* At the sampling site, fix a piece of nylon
156 mesh on the opening of the collection container (oxic water sampling) or attach the nylon mesh
157 to the tip of the sampling tube, submerged in the collection container (ferrous water sampling)
158 to filter out coarser material. The mesh size depends on practicalities; decide on a size range
159 which allows a decent flow of water through without clogging. We successfully used a 10 μm
160 nylon mesh for lake, stream and groundwater, collecting about 1 L per minute using a peristaltic
161 pump. *c)* Rinse the polyethylene container three times with sampling water before final filling.
162 When sampling ferrous water, oxygen could enter the anoxic sample and Fe-oxides could start
163 to precipitate. To avoid those processes rinse and fill the container by pumping water through
164 the submerged tube into the container and let the water overflow for an extended period of time.
165 At the final filling, prevent a headspace in the container before closing it. *d)* Collect a parallel
166 water sample (minimum 10 mL) for measurement of P_i concentration and $\delta^{18}\text{O}$ of water, i.e.
167 $\delta^{18}\text{O}_w$.



168 *Evaluation of the water sampling protocol*

169 So far, there is no clear guideline regarding the proper filtration requirement for freshwater
170 samples. However, the selected filtration procedure might have an effect on the final obtained
171 purified Ag_3PO_4 . If necessary particulate organic matter has typically been removed from freshwater
172 samples by filtration through a $0.45\ \mu\text{m}$ GF/F filter (Davies et al., 2014; Elsbury et al., 2009; Li et al.,
173 2011). However, it is extremely impractical to filter many litres of water through a 0.45 micron filter.
174 When working with freshwater samples, filtration of the HNO_3 solution after dissolution of the last
175 MagIC pellet (Step VI) could be a solution. Nevertheless, to our knowledge, this still needs to be
176 elucidated further.

177 *2.3. Quantitative P_i removal by the MagIC method*

178 The MagIC method was developed by Karl & Tien (1992) and later improved by Thomson-
179 Bulldis & Karl (1998) to precisely determine nanomolar concentrations of SRP and total dissolved
180 phosphorus from marine and freshwater ecosystems. The technique concentrates and isolates P_i from
181 the majority of other dissolved ions, and ideally also from DOP and DOM, thus enabling a more
182 manageable P_i sample for further treatment prior to the final Ag_3PO_4 precipitation.

183 **Step II. Magnesium-induced co-precipitation of dissolved P_i (MagIC)**

184 Magnesium-induced co-precipitation can quantitatively remove dissolved P_i by adsorption onto
185 $\text{Mg}(\text{OH})_2$ (brucite), initiated by addition of NaOH which raises the pH. This is utilized in the first step
186 of the MagIC approach. Brucite can precipitate at any temperature, but temperatures should be kept
187 low ($5\text{-}10^\circ\text{C}$) in order to keep microbial activity at a minimum. Microbial activity may alter the source
188 $\delta^{18}\text{O}_\text{P}$ signatures through biological uptake and recycling (Blake et al., 2005).

189 The procedure of the brucite precipitation step is as follows:

190 *a)* Discard some of the sampled water to ensure space for the reactants. *b)* Add 3 M Mg-brine to
191 the water sample in the polyethylene container. The required volume deviate according to the
192 sample volume. Add until the solution achieve a final concentration of $\sim 55\ \text{mM}$ Mg^{2+} (Karl &
193 Tien, 1992; Thomson-Bulldis & Karl, 1998); for example, this corresponds to the addition of 1 L
194 3 M Mg-brine to 50 L freshwater sample. Mix well. The required Mg^{2+} concentration stems from
195 an experimentally evaluated efficacy of P_i removal from Mg^{2+} -amended freshwater samples by
196 Karl & Tien (1992) and corresponds to the Mg^{2+} concentration found in seawater. *c)* Then add 1
197 M NaOH equivalent to 0.5% of the sample solution volume (Thomson-Bulldis & Karl, 1998) and
198 mix again. Check with pH indicator strips that the pH becomes between 9 and 10, as alkaline
199 conditions facilitate brucite precipitation better than acidic conditions (Thomson-Bulldis & Karl,

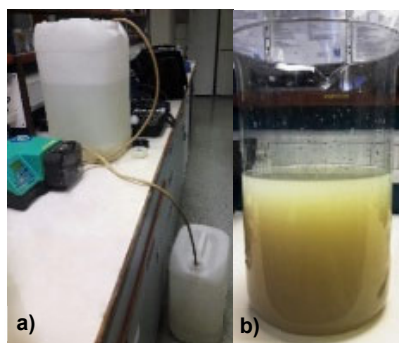


Figure 1. (a) Removing the supernatant from the brucite flocs by siphoning, using a peristaltic pump. (b) Brucite flocs left after discarding the supernatant.



200 1998). If $\text{pH} < 9$ add more 1 M NaOH and mix simultaneously. *Note* that excess NaOH does not
201 improve P_i co-precipitation removal because the resulting higher pH decreases PO_4 adsorption.
202 Rather, excess NaOH has the drawback that it yields a larger mass of brucite flocs which
203 subsequently must be dissolved in a larger volume of acid (Karl & Tien, 1992). *d*) Allow the
204 brucite flocs to settle by gravity over a couple of hours. Then remove the supernatant. If the
205 volume of the sample solution is large, this can be done by siphoning or using e.g. a peristaltic
206 pump (Figure 1a). The brucite flocs might make up several liters of sludge (Figure 1b). *Note* that
207 P_i may start to desorb from the brucite flocs, probably because recrystallization of the brucite
208 lowers the surface area if the suspension is left for longer than it takes the brucite flocs to settle
209 (Colman, 2002). *e*) Check the absence of P_i in the supernatant, e.g. by using the
210 spectrophotometric molybdate blue-method (Murphy & Riley, 1986). Discard the supernatant if
211 P_i has been 100% stripped from the sample solution. If P_i is still present, add additional 1 M
212 NaOH to the supernatant until no P_i can be detected; the supernatant at this point has a Mg
213 concentration still matching seawater (supported by PHREEQC modelling). Combine all the
214 precipitated brucite.

215 *Method disagreement* regarding the precipitation approach of brucite exists: Joshi et al. (2018) initially
216 prepared a concentrated MgCl_2 colloidal solution in a split of the sample solution (200–300 mL) and
217 concurrently adjusted the pH of the remaining sample solution. They then subsequently mixed the
218 two solutions. The entire volume was then gently shaken continuously to maintain a homogeneous
219 dispersion of colloids and thus maximize the trapping of P_i . Joshi et al. (2018) state that this procedure
220 is especially prudent when working with low P_i concentrations. This method procedure has
221 successfully been followed by Yuan et al. (2019). Whether there are discrepancies in the results if one
222 follows this approach instead of the magnesium-induced approach described in Step II is currently
223 undocumented.

224 **Step III. Sample centrifugation**

225 The brucite flocs can be separated from the solution by centrifugation. Do the following:

226 *a*) After completing Step II, immediately centrifuge the collected brucite floc sludge at 3500 rpm
227 for 10 minutes, and discard the supernatant. Timewise, it is recommended to use as large
228 centrifuge tubes as possible, e.g. 250 mL tubes. (No further substeps in Step III.)

229 *Method disagreement* regarding the recommended centrifugation rotation speed: Karl & Tien (1992)
230 recommend a low speed (1000 rpm for 1 h) as high g-forces (experienced at >12000 rpm; Karl & Tien,
231 1992) make the settled brucite flocs harder to dissolve subsequently and do not improve the
232 separation from the supernatant. In contrast, Goldhammer et al. (2011) recommends a high rotation
233 speed (10000 rpm for 15 minutes) to ensure complete settling of the fine crystalline $\text{Mg}(\text{OH})_2$. The
234 underlying reasoning for Goldhammer et al.'s approach is that the $\delta^{18}\text{O}_P$ of the P trapped in the fine
235 fraction is significantly different from the $\delta^{18}\text{O}_P$ of coarser brucite flocs. In practice, these fines are not
236 visible to the eye; the supernatant in either case should appear clear. The amount of associated P
237 therefore must remain tiny compared to the amount in the visibly settled flocs, meaning that the
238 difference in $\delta^{18}\text{O}_P$ needs to be comparably high. Nevertheless, we followed McLaughlin et al. (2004)'s
239 compromise where a rotational speed of 3500 rpm for 10 minutes was used. This approach was
240 successful followed by Young et al. (2009) and Elsbury et al. (2009), both working with freshwater
241 samples. An alternative to centrifugation is gravitational separation used by Colman (2002).

242 **Step IV. Brucite dissolution**

243 The co-precipitated P_i is re-liberated by dissolving the brucite flocs in 1 M HNO_3 . The technique is as
244 follows:

245 *a*) Add 1 M HNO_3 to the centrifuge tubes used for Step III. The required added volume deviate
246 according to the quantity of brucite flocs. Add until the brucite can be easily removed from the



247 centrifuge tubes. Be sure to use the minimum amount of acid to minimize acid hydrolysis (Karl
248 & Tien, 1992); elaborate explanation in section 2.3.1. *b*) Combine the dissolved brucite flocs from
249 the centrifuge tubes. *c*) Adjust the final pH to ca. 1 using 1 M HNO₃ (use indicator pH test strips),
250 as brucite is first fully dissolved under these conditions; at this point the solution will be liquid
251 and not viscous.

252 **Step V. Additional MagIC step**

253 If the sample contain organic material, the color of the precipitated brucite flocs become tan or even
254 brown (Goldhammer et al., 2011; Zohar et al., 2010) (Figure 2), whereas it should be milky whitish if
255 purified (Karl & Tien, 1992). An additional MagIC step, Step V, is thus required leading to *(i)* further
256 purification of P_i from a matrix with potential contaminants and *(ii)* higher concentrated P_i brucite
257 flocs (Colman, 2002; Goldhammer et al., 2011). Step V proceeds as follows:

258 *a*) Raise the pH of the dissolved brucite to about 10-11 by adding 1 M NaOH (do not add the
259 Mg-brine). Brucite precipitation occurs at pH 9. *b*) Then, repeat Step III and Step IV. *Note* that a
260 final pH of 1 is still required. *c*) Repeat Step V until discoloration disappears; up to five
261 repetitions may be necessary (Goldhammer et al., 2011).

262 *Method disagreement* exists regarding the final pH of the dissolved brucite solution. Colman (2002),
263 Goldhammer et al. (2011) and McLaughlin et al. (2004) all recommend carefully buffering the solution
264 back up to a pH between 4 and 6 after re-dissolution of the brucite is complete, making H₂PO₄⁻ the
265 main P_i species in the solution. McLaughlin et al. (2004) used 1 M potassium acetate as buffer as it is
266 inexpensive, nontoxic, and has a low P content, whereas Colman (2002) and Goldhammer et al. (2011)
267 used 1 M NaOH to adjust pH. However, the subsequent purification steps in these three studies
268 (precipitation of cerium phosphate (McLaughlin et al., 2004) and a pump-based anion-exchange
269 chromatography setup (Colman, 2002; Goldhammer et al., 2011)) differ from the purification step
270 presented in our protocol and they all utilize a pH of around 6. In this protocol the subsequent
271 purification steps utilize the low pH (see Step VII). Adjustment of pH is therefore not applied in the
272 MagIC protocol presented in the present study.

273 **Step VI. Filtration**

274 After completing Step V one should be left with a solution with a pH of ~1. The final step of the
275 MagIC protocol separates contaminants insoluble under acid conditions and not incorporated in the
276 brucite flocs, by vacuum filtration. Do the following:

277 *a*) Filtrate the dissolved brucite using a 0.7 μm GF/F filter. It may be necessary to centrifuge first
278 if the floc is not fully dissolved in acid at pH 1. (No further substeps in Step VI.)

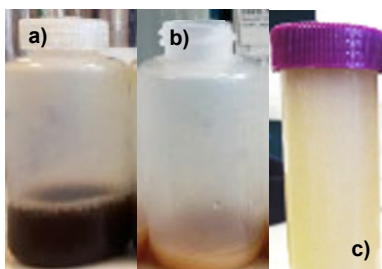


Figure 2. Brucite discoloration of sample with high dissolved organic matter (DOM) content. DOM-rich brucite flocs after (a) the first precipitation, (b) after three HNO₃ dissolution and NaOH precipitation repetitions and (c) purified brucite (Step V).



279 After this step, it is recommend to proceed with the the subsequent purification step (Step VII),
280 without waiting too long. If the samples needs to be stored and/or transported than do not dissolve
281 the brucite flocs after the last brucite precipitation and store the sample in the fridge. The brucite flocs
282 should first be dissolve in acid just before the first purification (Step VII).

283 *Evaluation of the MagIC protocol*

284 In general, we found the MagIC protocol to be an effective method to remove P_i from water
285 samples. It is, however, obligatory to check the P_i concentration in the supernatant generated in Step
286 II before it is discarded.

287 The MagIC protocol was initially developed for samples of seawater (Karl & Tien, 1992) which
288 has a nearly constant matrix composition independent of the sampling site and a naturally high
289 concentration of Mg^{2+} (55 mM). Also, seawater P_i concentrations are rarely high enough to challenge
290 the quantitative P_i removal in Step II. In contrast to seawater, when working with freshwater samples,
291 the matrix can vary significantly and Mg^{2+} needs to be added.

292 Karl & Tien (1992) conducted a limited preliminary investigation of the MagIC technique on
293 freshwater samples, were the results indicated its applicability. This was later substantiated by
294 Elsbury et al. (2009), Goldhammer et al. (2011) and McLaughlin et al. (2004). They all used the MagIC
295 technique for isolation of P_i in freshwater samples. Nonetheless, an initial incomplete quantitative
296 removal of P_i from the sample solution has been attributed the presence of HCO_3^- , as HCO_3^- has an
297 affinity for brucite similar to P_i , and thus reduces the P sorption capacity of brucite (Joshi et al., 2018).
298 An extra step prior to the MagIC treatment where HCO_3^- is removed by acid treatment forming
299 degassing CO_2 (Joshi et al., 2018) may thus be required; this was not attempted in the present study.

300 Additional amendments and additions to the MagIC protocol might be necessary when working
301 with some freshwater samples. This is an important subject, which still needs to be investigated in
302 more detail.

303 The acid dissolution of brucite can be a weakness for organic rich samples (i.e. Step IV). During
304 that step acid hydrolysis may occur, which may potentially convert organic P into new P_i in which
305 water-O from the ambient environment may be incorporated (McLaughlin et al., 2006). The newly
306 generated P_i will potentially be incorporated in the Ag_3PO_4 crystals, subsequently altering $\delta^{18}O_p$
307 signature of the sample. By repeating the MagIC step (cf. Step V) the samples are exposed for a longer
308 acid contact period and thus, there is a higher risk of isotopic alteration driven by acid hydrolysis.

309 Colman (2002), Thomson-Bulldis & Karl (1998), and Jaisi & Blake (2014) all experimentally
310 validated, that hydrolysis of a large range of DOP compounds is negligible at extreme (low and high)
311 pH in the time frame used in routine laboratory processing of samples. Furthermore all reported
312 hydrolysis impacts on $\delta^{18}O_p$ are below the analytical error (Paytan & McLaughlin, 2011). Yet it is
313 important to keep in mind the significant variation of the freshwater matrix, and thus the vast array
314 of organic P compounds with different affinities for the brucite flocs (Colman, 2002; Thomson-Bulldis
315 & Karl, 1998).

316 It is therefore wise to test samples that might be susceptible to acid hydrolysis (e.g. organic-rich
317 samples or samples with an anomalous composition of organic carbon) for isotopic contamination
318 driven from this mechanism. ^{18}O -labeled and unlabeled reagents on replicates of the same sample
319 can be used to trace and correlate the impact of acid hydrolysis.

320 The positive effect of minimizing the DOM content and other O-bearing compounds remaning
321 in the sample by repeating the MagIC step might exceed its negative impacts. As mentioned,
322 inefficient removal of O-bearing contaminating compounds, including DOM, nitrate (NO_3^-), sulphate
323 (SO_4^{2-}) and calcium carbonate ($CaCO_3$) could result in inclusion of O from other compounds than PO_4
324 in the precipitated Ag_3PO_4 (Davies et al., 2014; Lécuyer, 2004) and could thus significantly influence
325 the measured $\delta^{18}O_p$ signature. Especially DOM, containing up to 45% O by weight has been shown
326 to persist until the precipitation of Ag_3PO_4 (McLaughlin et al., 2004). In literature, remaining O-
327 bearing compounds potentially being incorporated into the Ag_3PO_4 seems to be of bigger concern
328 (Davies et al., 2014; Goldhammer et al., 2011; Gruau et al., 2005; McLaughlin et al., 2004; Tamburini



329 et al., 2010) than the probability of acid hydrolysis during brucite dissolution (Jaisi & Blake, 2014;
330 Paytan & McLaughlin, 2011).

331 An alternative to the MagIC protocol is the quantitative removal of P_i by co-precipitation with
332 Fe-oxides (Longinelli et al., 1976) which has been proven successful for freshwater samples (Gruau
333 et al., 2005; Neidhardt et al., 2018). Fe-oxide co-precipitation is initiated by addition of 0.1 M $FeSO_4$
334 accompanied with aeration of the sample at a pH of 8.5 ± 0.1 (optimal for Fe-oxide precipitation; Gruau
335 et al., 2005). Neidhardt et al. (2018) found that it is not necessary to add $FeSO_4$ if the initial dissolved
336 Fe^{2+} concentration in the solution samples are high (>1 mg Fe^{2+}/L). It still needs to be investigated
337 which which of the two approaches for quantitative P_i removal is preferable.

338 2.4. Purification and silver phosphate precipitation

339 The phosphate purification protocol presented in the present study is based on the method
340 published by Tamburini et al. (2010). The advantage of Tamburini et al. (2010)'s protocol is that it was
341 developed with the specific goal of minimizing the effect of organic matter on $\delta^{18}O_p$. Tamburini et al.
342 (2010)'s purification steps of sequential precipitation and recrystallization were adapted from
343 Kolodny et al. (1983) and modified by Liang & Blake (2006). Briefly, P_i is first precipitated as
344 ammonium phospho-molybdate (APM), and then recrystallized as magnesium ammonium
345 phosphate (MAP). This is combined with a subsequent cation resin treatment followed by elimination
346 of chloride. The purification protocol is presented below.

347 Step VII. Ammonium phospho-molybdate (APM) precipitation

348 During the first step of the purification protocol, P_i is scavenged from the acidic dissolved brucite
349 solution by precipitation of APM crystals. This enables the separation and removal of ions and
350 contaminants that are soluble at low pH (Joshi et al., 2018). The APM precipitation procedure is as
351 follows:

352 a) Initially, transfer the sample solution (i.e. the dissolved brucite) to an Erlenmeyer flask of
353 suitable volume (sample and reactants combined volume) and place the flask in a 50 °C warm
354 water bath shaker or on a magnetic stirrer with heating set to 50 °C. b) If the solution is taken
355 directly from the refrigerator, wait until the sample is close to room temperature before
356 continuing. c) Then add 25 mL 35% ammonium nitrate reagent, and then slowly add 40 mL of
357 the 10% NH_4 -molybdate solution. d) Adjust the final pH to ca. 1 using 1 M H_2SO_4 , (use indicator
358 pH test strips). Normally around 1 mL is enough; thereby the volume of the sample is not
359 affected too much. Note that if the supernatant turns transparent bright yellow (Figure 3a) this
360 is an indication that optimal precipitation condition with respect to APM crystals are obtained.
361 When this color changes to milky yellow, it indicates that APM crystals are forming (Figure 3b).
362 If no APM crystals have started to precipitate from the heated solution (> 25 °C) after around 15
363 min, supersaturated conditions with respect to APM crystals are likely not obtained or pH is not
364 correctly adjusted. First check the pH and adjust if necessary. If still no APM crystals precipitate,
365 add stepwise more 35% ammonium nitrate and 10% NH_4 -molybdate solution in the same ratio
366 as before (2.5:4) until signs of crystal precipitation. e) Leave the solution in the 50 °C warm water
367 bath and shake gently overnight to ensure complete APM precipitation.

368
369 We experienced that if the supernatants were slightly alkaline after Step VIIc it became bright green
370 (Figure 3c) and no APM started to precipitate. When adjusting the pH to 1 the supernatant turned to
371 a transparent bright yellow color (Figure 3a) and APM crystal immediately began to form. The
372 slightly alkaline condition could have affected the dissolution of the brucite flocs, since brucite
373 dissolve at acidic conditions flocs. We also experienced that if the brucite flocs had not been acidified
374 to pH 1 during the dissolution step (Step IV) and/or the additional MagIC step (Step V) was not
375 conducted, the crystals precipitating in this purification step were white and the supernatant
376 transparent (Figure 3d). Furthermore, we were not able to accomplish a final precipitation of Ag_3PO_4
377 when we tried to proceed with these white crystals. Accordingly, we suggest that the color of the

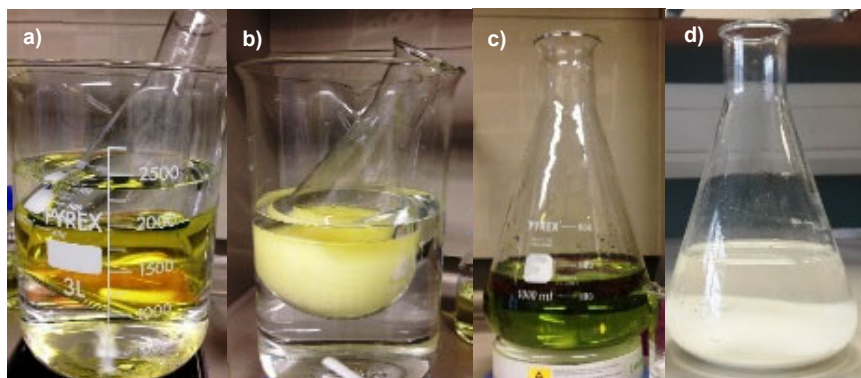


Figure 3. Color of the supernatant and the precipitate in Step VII when (a) optimal precipitation condition with respect to APM crystals are obtained, (b) APM crystals are forming, (c) alkaline condition which impede APM precipitation and (d) with an unidentified precipitate resulting from incorrect execution of the MagIC protocol (section 2.3).

378 supernatant and the precipitate can be used as an indicator for (i) optimal pH conditions for APM
379 precipitation and (ii) whether it is worthwhile to continue. The adjustment of the pH and an
380 introduction of additional MagIC steps were performed simultaneously in the present study. No
381 examination of whether both actions are equally important has been reported nor tested in the
382 present study.

383

384 **Step VIII. APM dissolution**

385 The P_i is released from APM by dissolution of the crystals in an alkaline solution prior to an additional
386 purification step. Conduct the step as follows:

- 387 a) Start by separating the yellow APM crystals from the supernatant by vacuum filtration upon
388 a $0.2\ \mu\text{m}$ cellulose acetate filter and discard the supernatant. The filtration time can take several
389 hours and more than one filter may be necessary. APM crystals from different samples may
390 differ slightly from each other in color and size (Figure 4). b) Wash the crystals thoroughly with
391 a 5% ammonium nitrate solution to rinse off contaminants. The more, the better ($>200\ \text{mL}$). c)
392 Transfer the filter containing the APM crystals to a 100 mL Erlenmeyer flask and place the flask



Figure 4. Vacuum filtered and 5% ammonium nitrate washed ammonium phosphomolybdate crystals (APM) from two different samples. The APM crystals differ in color and size.

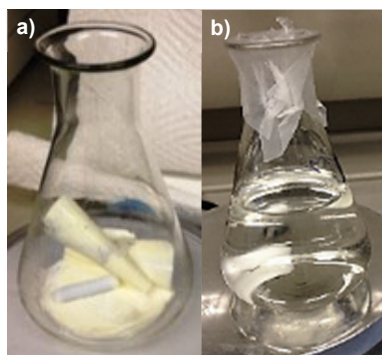


Figure 5. a) Ammonium phosphomolybdate crystals (APM) on $0.2\ \mu\text{m}$ cellulose acetate filters. b) Dissolved APM crystal in a NH_4 -citrate solution resulting in a transparent solution.



Figure 6. Greenish discoloration of the dissolved ammonium phosphomolybdate crystals.



Figure 7. Precipitated magnesium ammonium phosphate crystals .

393 on a magnetic stirrer. *d*) Dissolve the APM crystals in a minimum amount of NH_4 -citrate solution
394 (15-50 mL; volume depends on the quantity of formed APM crystals). Start by adding 10 mL and
395 then add 5 mL aliquots. Work under a chemical fume hood. *e*) Gently swirl the solution while
396 the crystals are dissolving and wait until the solution becomes transparent (Figure 5), which may
397 take up to 15-20 minutes. Then remove and discard the filter(s). *Note* that Mg^{2+} ions could
398 interfere with dissolution of the APM crystals leading to some crystals not dissolving. In
399 addition, silicates may have formed in the former steps. These are not dissolvable in the NH_4 -
400 citrate solution. Accordingly, some particulate compounds might be left in the solution after it
401 turns transparent. If so, filter again using a $0.2\ \mu\text{m}$ cellulose nitrate filter and discard the filter.

402 *We experienced* that the dissolved APM solution at times had a greenish discoloration, maybe due
403 to precipitation formation of silicate molybdate complexes (Figure 6). This could possibly indicate
404 that silicate molybdate complexes have formed. We tried to continue the protocol with these samples
405 which still resulted in Ag_3PO_4 crystal precipitation in the last step.

406 **Step IX. Magnesium ammonium phosphate (MAP) precipitation**

407 In this step P_i is further purified by precipitating MAP crystals under alkaline conditions, thus
408 enabling the removal of ions and contaminants that are soluble at high pH. The MAP precipitation
409 procedure is as follows:

410 *a*) Initially add 25 mL Mg-reagent to the 100 mL Erlenmeyer flask, containing the dissolved
411 APM solution, while stirring. *b*) Then slowly add about 7 mL of the 1:1 ammonia solution. *c*)
412 Check pH. If $\text{pH} < 8$ carefully add more of the 1:1 ammonia solution until the solution acquires
413 $\text{pH} 8-9$ which is the optimum pH for MAP precipitation. MAP crystals should start to
414 precipitate immediately, turning the solution whitish opaque (Figure 7). *d*) Cover the
415 Erlenmeyer flask with parafilm and make mm-size holes for venting. Leave the solution
416 overnight on the magnetic stirrer.

417 *We experienced* that it was necessary to add a bit more Mg-reagent to some of the samples, after
418 adjusting pH to 8-9, in order to achieve supersaturation with respect to the MAP crystals. This was
419 true for the samples where $>20\ \text{mL}$ of NH_4 -citrate solution had been used to dissolve the APM
420 crystals.

421 **Step X. MAP dissolution**

422 P_i is released by dissolving the MAP crystals in a minimum amount of HNO_3 .

423 *a*) Separate the white MAP crystals from the supernatant by vacuum filtration upon a $0.2\ \mu\text{m}$
424 cellulose nitrate filter and discard the supernatant. The MAP crystals are small and may be quite



425 hard to see on the filter by eye, see Figure 8. *b*) Wash the crystals thoroughly with 1:20 ammonia
426 solution (>200 mL) to get rid of excess chloride and other contaminants. *Note* that this is of
427 extreme importance as remaining Cl^- from the Mg solution (i.e. MgCl_2 and HCl) will cause co-
428 precipitation of AgCl during the final precipitation of Ag_3PO_4 . *c*) Transfer the filter to a 50 mL
429 centrifuge tube (with lid) and dissolve the MAP crystals in a minimum amount of 0.5 M HNO_3
430 (5-10 mL) by shaking the sample. *d*) Leave the filter in contact with the acid for at least 15-20
431 minutes to ensure that the MAP has dissolved. *Note* that it is difficult to assess when the crystal
432 have fully dissolved, since the filters and the crystals are both white.

433 Step XI. Cation removal

434 The presence of cations (primarily Na^+ and multivalent cations such as Mg^{2+}) interferes with the
435 precipitation of Ag_3PO_4 . Thus a prior cation removal step is a crucial prerequisite for the subsequent
436 successful precipitation of purified Ag_3PO_4 (Firsching, 1961). Cations can be scavenged by a proton-
437 charged cation resin, releasing H^+ to solution, which subsequently reacts with HCO_3^- (if present),
438 forming H_2O and CO_2 (Colman, 2002). The purification step is as follows:

439 *a*) Convert the new cation exchange resin AG50WX8 to an H^+ form by reacting the resin with 7
440 M HNO_3 overnight, on a horizontal shaker. A 7 M HNO_3 volume equivalent to 1.5 times the
441 resin volume is recommended. *b*) The following day discard the HNO_3 and rinse the resin
442 thoroughly by mixing it with 1 L DD- H_2O to bring it close to neutrality (>5). *c*) Filtrate the
443 mixture on a 0.45 μm polycarbonate filter and discard the water. It might take up to several
444 repetitions before a neutral pH is obtained. *d*) Add 6 mL of the obtained cation resin slurry to
445 the sample solution. Seal the sample with a lid or parafilm and place the sample on a shaker
446 overnight. *e*) The next day, filter the sample using a 0.2 μm polycarbonate filter and rinse the
447 cation resin with 1-2 mL DD- H_2O . *f*) Collect the resin and recondition it in 1 M HNO_3 . The resin
448 can be re-used.

449 *Method disagreement* regarding the preparation of the cation resin. Goldhammer et al. (2011)
450 experienced a reddish discoloration of the sample when using resin prepared the previous day.
451 Subsequently they were unable to properly precipitate Ag_3PO_4 . By preparing the cation resin within
452 30 min of its use they avoided this problem. They did not resolve the cause of this complication. We
453 experienced that the samples acquired a milky white color once the resin was added, if the resin was
454 prepared two days before its use (our resin was left in DD- H_2O overnight). The whitish coloration
455 was avoided when using the resin the same day as it was washed in DD- H_2O . It was not possible to
456 properly precipitate Ag_3PO_4 when using samples where the milky white color had occurred. Thus,
457 we agree with Goldhammer et al. (2011)'s statement, that proper handling and rinsing of the resin
458 before every application is crucial to the successful precipitation of Ag_3PO_4 .

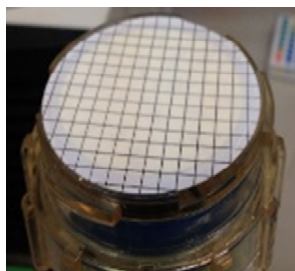


Figure 8. Vacuum filtered and 1:20 ammonia solution washed magnesium ammonium phosphate crystals.



Figure 9. Precipitated AgCl crystals after adding AgNO₃ to the sample solution.

459 Joshi et al. (2018) adjusted the pH of the dissolved MAP solution to neutral (pH 6-8) prior to the
460 cation removal.

461 **Step XII. Elimination of Cl⁻**

462 Removal of Cl⁻ ions is extremely important, as Cl⁻ otherwise may react with the Ag⁺ in the final
463 precipitation of Ag₃PO₄, forming AgCl which have been observed to be rimmed by silver oxide
464 precipitates (Colman, 2002). Precipitation of AgCl hence both interfere with the Ag₃PO₄ precipitation
465 (McLaughlin et al., 2004) and introduce non-phosphate oxygen to the sample (Colman, 2002).
466 Chloride can be quantitatively removed by adding AgNO₃ crystals to the sample when the pH is
467 acidic, causing AgCl precipitation (Figure 9) prior to the Ag₃PO₄ precipitation step. The low pH in
468 the sample (<1) impede co-precipitation of Ag₃PO₄, and hence no P_i is lost during this step. The
469 purification step is as follows:

470 *a)* Transfer the filtrated sample solution to a small container with a small opening (e.g. 50 mL
471 centrifuged tube) *b)* Add a few AgNO₃ crystals to the sample solution. If the sample turns
472 whitish opaque AgCl has precipitated (Figure 9). *d)* Wait at least 5 minutes and re-filter, the same
473 filter used in Step XI can be re-used.

474 After this purification step, the initial freshwater sample with a volume up to 50 L has been reduced
475 to about 10 mL highly concentrated homogeneous P_i solution stripped of potential contaminants. The
476 sample is now ready for the final Ag₃PO₄ precipitation.

477 **Step XIII. Silver phosphate (Ag₃PO₄) precipitation**

478 Precipitation of insoluble silver salts, such as Ag₃PO₄, can be conducted by volatilization of ammonia
479 (Firsching, 1961). This allows a 'slow' recrystallization which facilitates the growth of large and
480 easier-to-handle Ag₃PO₄ crystals for oxygen isotope analysis by IRMS within a few days (Firsching,
481 1961; Goldhammer et al., 2011). The method utilizes that Ag₃PO₄ precipitates in the solution at a pH
482 around 7±0.5 when free Ag⁺ and P_i are present. Thus the pH conditions and a high Ag⁺:P_i ratio is of
483 extreme importance to ensure complete precipitation of Ag₃PO₄. The 'slow' Ag₃PO₄ precipitation
484 procedure is as follows:

485 *a)* Initially add the Ag-ammine solution to the sample solution, in a Ag:P_i ratio of approximately
486 10:1 (Colman, 2002). The sample solution turns briefly white (at pH 7), and then transparent (at
487 pH>7) once the alkaline Ag-ammine solution has been added. *b)* The sample container is then
488 placed in an oven at 50 °C. Yellow Ag₃PO₄ crystals start to precipitate after a few hours as the
489 amine starts to vaporize and the Ag⁺ is released (Firsching, 1961). Complete precipitation of the
490 crystals takes up to two days. *Note* that it impotent to repeatedly add DD-H₂O to the solution to
491 keep the volume as constant as possible. If left unattended (e.g. for one or several days) all the
492 H₂O may evaporate, which results in uncontrolled precipitation of salts. This is still fine, as the



493 salts will be dissolved when adding DD-H₂O, as they are mostly nitrate-based. If this happen it
494 is vital to wash the Ag₃PO₄ crystals easterly well with DD-H₂O. The small diameter of the tube
495 and the low temperature of the oven, impedes the evaporation ammonia, and thus enables a
496 slow crystallization process (Colman, 2002). *c*) After 1 to 2 days, if no yellow Ag₃PO₄ crystals
497 have precipitated, check the pH of the solution. If the pH of the solution differs from pH 7
498 (optimal pH for Ag₃PO₄ precipitation conditions; Firsching, 1961) adjust the pH by adding either
499 HNO₃ or NH₄OH. *Note* that under no circumstances should HCl or NaOH be used to adjust the
500 pH as Cl⁻ and Na⁺ would interfere with the crystallization of Ag₃PO₄. *d*) When crystals have
501 formed, vacuum filter them upon a 0.2 μm polycarbonate filter and discard the supernatant.
502 Other filters tend to ‘trap’ the Ag₃PO₄ crystals on their surface. *Note* that Ag₃PO₄ crystals may
503 form on the side of the tube, hence make sure to carefully detach these and transfer them to the
504 filter as well. *e*) Wash the crystals extremely thoroughly with DD-H₂O to get rid of residual O-
505 bearing compounds, as they interfere with the oxygen isotope analysis (cf. Section 2.3.1). *f*) Place
506 the filter on a Petri dish and cover it to prevent contamination and loss of crystals. Dry the filter
507 at 50 °C for at least 1 day. *g*) An extra elimination of residual organic matter might be necessary
508 by introducing a final washing of the Ag₃PO₄ precipitate with hydrogen peroxide to eliminate
509 residual organic matter by oxidation (Tamburini et al., 2010). *Note* that Crowson et al. (1991)
510 found that contaminated silver phosphate crystals were generally dark brown to greenish brown
511 in color and cohesive. We did not experience this discoloration but the crystal became dark
512 under light, probably do to the photo-oxidation of silver (McLaughlin et al., 2004; Tamburini et
513 al., 2010). *h*) If needed, the filter containing the Ag₃PO₄ crystals can be stored in a desiccator.

514 *Method disagreement* regarding the Ag₃PO₄ precipitation rate. The final precipitation of Ag₃PO₄ can be
515 accomplished by either a ‘slow’ (Goldhammer et al., 2011; Tamburini et al., 2010) or ‘fast’ (Dettman
516 et al., 2001; McLaughlin et al., 2004) precipitation method. In contrast to the ‘slow’ method presented
517 in the present protocol, ‘fast’ AgNO₃ precipitation is achieved by first altering the solution pH to 7 by
518 adding NH₄OH, NH₄NO₃ and nitric acid (HNO₃). Then follows the addition of AgNO₃ crystals
519 dissolved in DD-H₂O, which initiate a rapid precipitation of Ag₃PO₄ within a few minutes
520 (McLaughlin et al., 2004).

521 Dettman et al. (2001) compared the isotopic composition of the Ag₃PO₄ generated by the two
522 different methods and found the resulting δ¹⁸O_p values to be within expected interlaboratory
523 variation. Tamburini et al. (2010) suggest, however, using the ‘slow’ precipitation method as an
524 additional measure to minimize the disturbance by organic matter as suggested by Colman (2002).



Figure 10. A microplate, used for transportation of
timble capsules containing Ag₃PO₄ crystals.



525 **Step XIV. Ag_3PO_4 crystal preparation prior to isotope ratio mass spectrometry (IRMS)**

526 Once the Ag_3PO_4 crystals have been precipitated, dried and stored in plastic vials they are prepared
527 for isotope ratio mass spectrometry (IRMS) analysis. Such sample preparation involves:

528 *a)* Weighing of $\sim 300 \mu\text{g}$ of Ag_3PO_4 crystals in triplicate from the plastic storage vial into silver
529 timble capsules. *b)* After weighing the Ag_3PO_4 and recording the weight, add a small amount
530 (few grains) of black carbon (no need to weigh this) to each sample. *c)* Close the capsules tight
531 by using tweezers but absolutely do not touch them with the fingers. *d)* Place the capsules in a
532 microplate with holes (Figure 10). Once all the samples have been weighed off, seal the plate. To
533 do this, cover the plate with parafilm, close it with the cover lid, and then fix the lid with tape.

534 The Ag_3PO_4 crystal are now ready to be shipped for $\delta^{18}\text{O}_p$ analysis.

535 *Evaluation of phosphate purification and silver phosphate precipitation*

536 The effectiveness of the different purification steps, in producing adequately pure Ag_3PO_4 , is
537 difficult to evaluate during the execution. Oxygen contamination can not be checked for until $\delta^{18}\text{O}_p$
538 has been analyzed. The oxygen yield of the sample is compared to that of the pure Ag_3PO_4 used as
539 standard (Tamburini et al., 2010). Therefore, it is important to know and pay attention to the
540 characteristics of the precipitated crystals in each step (e.g. correct crystal color) and evaluate whether
541 the specific purpose of the step has been obtained (e.g. whether crystals are formed or completely
542 dissolved).

543 **3. Final remarks**

544 In general, it is important to keep in mind, that the amount of added reactants and chemicals
545 can vary from water sample to water sample and in many instances it depends on yield volume or
546 quantity from the prior step. Hence, only minimum and indicative quantities are stated in the present
547 protocol.

548 As stated in the introduction, a variety of approaches have been attempted to address the
549 problem regarding $\delta^{18}\text{O}_p$ contamination resulting from O-bearing compounds others than P_i , and
550 from Na^+ , Cl^- and multivalent cations. Bearing in mind that many methods have been tested on
551 various water matrix compositions, their effectiveness may not be reproducible for all water samples
552 matrices. In order to achieve progress in developing and applying $\delta^{18}\text{O}_p$ to trace P sources and cycling
553 in freshwater ecosystems, a better understanding of the different methods' reliance on different water
554 matrices is crucial. This does not only apply to the purification steps but applies for all sections
555 presented in the present study.

556 In general, studies which have used $\delta^{18}\text{O}_p$ as a tracer emphasize the importance of additional
557 research and knowledge regarding $\delta^{18}\text{O}_p$ data for various potential phosphate sources especially for
558 freshwater systems (Elsbury et al., 2009; Granger et al., 2017; Tamburini et al., 2014; Young et al.,
559 2009). The detailed protocol provided in this study will hopefully contribute to enable a broader use
560 of $\delta^{18}\text{O}_p$ signatures as such a tracing tool.

561
562

563 **Competing interests** The authors declare to have no competing interests.

564

565 **Acknowledgements** The authors thank Jörg Lewandowski (IGB, Berlin) for helpful comments
566 to an early version of the manuscript. This study was funded by the Geocenter Denmark-grant 6-
567 2015.

568



569 Appendix A: Description of the preparation of all used reagents

570

571

Reagents used in Section 2.3:

572

• **3 M Mg-brine:** Dissolve 610 g $\text{MgCl}_2 \cdot 6\text{H}_2\text{O}$ (hexahydrate; MW 203.3 g/mol) in deionized distilled water (DD- H_2O) to a total volume of 1 L. After the salt has dissolved, filter the brine on a GF/F filter. The solution can be stored indefinitely.

573

574

575

• **1 M NaOH:** Dissolve 40 g NaOH pellets in deionized distilled water (DD- H_2O) to a total volume of 1 L. The solution can be stored indefinitely.

576

577

• **1 M HNO_3 :** Add 66 mL of concentrated HNO_3 to 934 mL of DD- H_2O . The solution can be stored indefinitely.

578

579

580

Reagents used in Section 2.4:

581

• **35% ammonium nitrate reagent:** Dissolve 538.5 g ammonium nitrate salt (MW 80.052 g/mol) in 1000 mL DD- H_2O . Stir well to dissolve the salt completely. The solution can be stored.

582

583

• **5% ammonium nitrate reagent:** Dissolve 105.5 g ammonium nitrate salt in 2000 mL DD- H_2O . Stir well to dissolve the salt completely. The solution can be stored.

584

585

• **10% NH_4 -molybdate solution:** This solution has to be prepared freshly by dissolving 53.3 g of ammonium molybdate salt (tetrahydrate form: 1235.86 g/mol) in 480 mL of DD- H_2O (enough for approximately 12 samples). The solution CANNOT be stored.

586

587

• **Ammonium-citrate solution:** Add 300 mL of DD- H_2O and 140 mL of concentrated NH_4OH to 10 g of citric acid while working under a chemical fume hood. The solution is stable at room temperature and can be stored.

588

589

• **Mg-reagent:** Dissolve 50 g of MgCl_2 (hexa-hydrate salt, MW 203.3 g/mol) and 100 g of NH_4Cl (MW 53.49 g/mol) in 500 mL DD- H_2O . Subsequently acidify the mixture to pH 1 with concentrated HCl. Finally, adjust the volume to 1 L with DD- H_2O . The solution is stable indefinitely and can thus be stored.

590

591

• **1:1 and 1:20 ammonia solutions:** Measure in a volumetric cylinder concentrated NH_4OH (50 mL for the 1:1 and 100 mL for the 1:20). Pour into an appropriate glass bottle and dilute with DD- H_2O (50 mL for the 1:1 and 1900 mL for the 1:20). The solution can be stored.

592

593

• **0.5 N HNO_3 solution:** Add 33 mL of concentrated HNO_3 to 967 mL of DD- H_2O . The solution can be stored.

594

595

• **Ag-ammine solution:** Dissolve 10.2 g of AgNO_3 salt (MW 169.87 g/mol) and 9.6 g of NH_4NO_3 in 81.5 mL of DD- H_2O . Subsequently add 18.5 mL of concentrated NH_4OH . The solution can be stored in the dark in an amber bottle.

596

597

598

599

600

601

602

603

604 4. References

605

Blake, R. E., O'Neil, J. R., & Garcia, G. A. (1997). Oxygen isotope systematics of biologically mediated reactions of phosphate: I. Microbial degradation of organophosphorus compounds. *Geochimica et Cosmochimica Acta*, 61(20), 4411–4422. [https://doi.org/10.1016/S0016-7037\(97\)00272-X](https://doi.org/10.1016/S0016-7037(97)00272-X)

606

607

Blake, R. E., O'Neil, J. R., & Surkov, A. V. (2005). Biogeochemical cycling of phosphorus: Insights from oxygen isotope effects of phosphoenzymes. *American Journal of Science*, 305(6–8), 596–620.

608

609

<https://doi.org/10.2475/ajs.305.6-8.596>

610

611

Colman, A. S. (2002). *The oxygen isotope composition of dissolved inorganic phosphate and the marine phosphorus cycle. Ph.D. thesis, Yale University, New Haven, CT.*

612

613

Crowson, R. A., Showers, W. J., Wright, E. K., & Hoering, T. C. (1991). Preparation of Phosphate Samples for Oxygen Isotope Analysis. *Analytical Chemistry*, 63(20), 2397–2400. <https://doi.org/10.1021/ac00020a038>

614

615

Davies, C. L., Surrridge, B. W. J., & Gooddy, D. C. (2014). Phosphate oxygen isotopes within aquatic ecosystems: Global data synthesis and future research priorities. *Science of the Total Environment*, 496, 563–575.

616

617

<https://doi.org/10.1016/j.scitotenv.2014.07.057>

618

619

Dettman, D. L., Kohn, M. J., Quade, J., Ryerson, F. J., Ojha, T. P., & Hamidullah, S. (2001). Seasonal stable isotope evidence for a strong Asian monsoon. *Geology*, 29(1), 31–34. <https://doi.org/10.1130/0091->



- 620 7613(2001)029<0031
- 621 Elsbury, K. E., Paytan, A., Ostrom, N., Kendall, C., Young, M., McLaughlin, K., et al. (2009). Using Oxygen
622 Isotopes of Phosphate To Trace Phosphorus Sources and Cycling in Lake Erie. *Environmental Science &*
623 *Technology*, 43(9), 3108–3114.
- 624 Firsching, F. H. (1961). Precipitation of Silver Phosphate from Homogeneous Solution. *Analytical Chemistry*, 33(7),
625 873–874. <https://doi.org/10.1021/ac60175a018>
- 626 Goldhammer, T., Max, T., Brunner, B., Einsiedl, F., & Zabel, M. (2011). Marine sediment pore-water profiles of
627 phosphate $\delta^{18}\text{O}$ using a refined micro-extraction. *Limnology and Oceanography Methods*, 9, 110–120.
- 628 Granger, S. J., Heaton, T. H. E., Pfahler, V., Blackwell, M. S. A., Yuan, H., & Collins, A. L. (2017). The oxygen
629 isotopic composition of phosphate in river water and its potential sources in the Upper River Taw
630 catchment, UK. *Science of the Total Environment*, 574, 680–690. <https://doi.org/10.1016/j.scitotenv.2016.09.007>
- 631 Gruau, G., Legeas, M., Riou, C., Gallacrier, E., Martineau, F., & Hénin, O. (2005). The oxygen isotope composition
632 of dissolved anthropogenic phosphates: A new tool for eutrophication research? *Water Research*, 39(1), 232–
633 238. <https://doi.org/10.1016/j.watres.2004.08.035>
- 634 Hecky, R. E., & Kilham, P. (1988). Nutrient limitation of phytoplankton in freshwater and marine environments:
635 A review of recent evidence on the effects of enrichment1. *Limnology and Oceanography*, 33(4, part 2), 796–
636 822. <https://doi.org/10.4319/lo.1988.33.4part2.0796>
- 637 Heiberg, L., Koch, C. B., Kjaergaard, C., Jensen, H. S., & Hans Christian, B. H. (2012). Vivianite Precipitation and
638 Phosphate Sorption following Iron Reduction in Anoxic Soils. *Journal of Environment Quality*, 41(3), 938.
639 <https://doi.org/10.2134/jeq2011.0067>
- 640 Jaisi, D. P., & Blake, R. E. (2014). *Advances in Using Oxygen Isotope Ratios of Phosphate to Understand Phosphorus*
641 *Cycling in the Environment. Advances in Agronomy* (1st ed., Vol. 125). Elsevier Inc.
642 <https://doi.org/10.1016/B978-0-12-800137-0.00001-7>
- 643 Jaisi, D. P., Kukkadapu, R. K., Stout, L. M., Varga, T., & Blake, R. E. (2011). Biotic and abiotic pathways of
644 phosphorus cycling in minerals and sediments: Insights from oxygen isotope ratios in phosphate.
645 *Environmental Science and Technology*, 45(15), 6254–6261. <https://doi.org/10.1021/es200456e>
- 646 Joshi, S. R., Li, W., Bowden, M., & Jaisi, D. P. (2018). Sources and Pathways of Formation of Recalcitrant and
647 Residual Phosphorus in an Agricultural Soil. *Soil Systems*, 2(3), 45.
648 <https://doi.org/10.3390/soilsystems2030045>
- 649 Karl, D. M., & Tien, G. (1992). MAGIC: A sensitive and precise method for measuring dissolved phosphorus in
650 aquatic environments. *Limnology and Oceanography*, 37(1), 105–116.
651 <https://doi.org/10.4319/lo.1992.37.1.0105>
- 652 Kolodny, Y., Luz, B., & Navon, O. (1983). Kolodny et al 1983, 64, 398–404.
- 653 Lécuyer, C. (2004). Oxygen Isotope Analysis of Phosphate. *Analysis*, 3(1983).
- 654 Li, X., Wang, Y., Stern, J., & Gu, B. (2011). Isotopic evidence for the source and fate of phosphorus in Everglades
655 wetland ecosystems. *Applied Geochemistry*, 26(5), 688–695. <https://doi.org/10.1016/j.apgeochem.2011.01.027>
- 656 Liang, Y., & Blake, R. E. (2006). Oxygen isotope signature of P: regeneration from organic compounds by
657 phosphomonoesterases and photooxidation. *Geochimica et Cosmochimica Acta*, 70(15), 3957–3969.
658 <https://doi.org/10.1016/j.gca.2006.04.036>
- 659 Longinelli, A. (1966). Ratios of oxygen-18:oxygen-16 in phosphate and carbonate from living and fossil marine
660 organisms. *Nature*, 211(5052), 923–927. <https://doi.org/10.1038/211923a0>
- 661 Longinelli, A., & Nuti, S. (1973a). Oxygen isotope measurements of phosphate from fish teeth and bones. *Earth*
662 *and Planetary Science Letters*, 20, 337–340.
- 663 Longinelli, A., & Nuti, S. (1973b). Revised phosphate-water isotopic temperature scale. *Earth and Planetary Science*
664 *Letters*, 19(3), 373–376. [https://doi.org/10.1016/0012-821X\(73\)90088-5](https://doi.org/10.1016/0012-821X(73)90088-5)
- 665 Longinelli, A., Bartelloni, M., & Cortecchi, G. (1976). The isotopic cycle of oceanic phosphate, I. *Earth and Planetary*
666 *Science Letters*, 32(2), 389–392. [https://doi.org/10.1016/0012-821X\(76\)90079-0](https://doi.org/10.1016/0012-821X(76)90079-0)
- 667 Marion, L., Clergeau, P., Brient, L., & Bertru, G. (1994). The importance of avian-contributed nitrogen (N) and
668 phosphorus (P) to Lake Grand-Lieu, France. *Hydrobiologia*, 279–280(1), 133–147.
669 <https://doi.org/10.1007/BF00027848>
- 670 McLaughlin, K., Silva, S., Kendall, C., Stuart-Williams, H., & Paytan, A. (2004). A precise method for the analysis
671 of $\delta^{18}\text{O}$ of dissolved inorganic phosphate in seawater. *Limnology and Oceanography: Methods*, 2(7), 202–212.
672 <https://doi.org/10.4319/lom.2004.2.202>
- 673 McLaughlin, K., Paytan, A., Kendall, C., & Silva, S. (2006). Oxygen isotopes of phosphatic compounds -
674 Application for marine particulate matter, sediments and soils. *Marine Chemistry*, 98(2–4), 148–155.
675 <https://doi.org/10.1016/j.marchem.2005.09.004>
- 676 McLaughlin, K., Kendall, C., Silva, S. R., Young, M., & Paytan, A. (2006). Phosphate oxygen isotope ratios as a
677 tracer for sources and cycling of phosphate in North San Francisco Bay, California. *Journal of Geophysical*



- 678 *Research: Biogeosciences*, 111(3), 1–12. <https://doi.org/10.1029/2005JG000079>
- 679 Moorleghem, V. C., De Schutter, N., Smolders, E., & Merckx, R. (2013). The bioavailability of colloidal and
680 dissolved organic phosphorus to the alga *Pseudokirchneriella subcapitata* in relation to
681 analyticalHydrobiologia phosphorus measurements. *Hydrobiologia*, 709(1), 41–53.
682 <https://doi.org/10.1007/s10750-013-1442-8>
- 683 Murphy, J., & Riley, J. P. (1986). A modified single solution method for the determination of phosphate in natural
684 waters. *Analytica Chimica Acta*, 27, 31–36. [https://doi.org/10.1016/S0003-2670\(00\)88444-5](https://doi.org/10.1016/S0003-2670(00)88444-5)
- 685 Neidhardt, H., Schoeckle, D., Schleinitz, A., Eiche, E., Berner, Z., Tram, P. T. K., et al. (2018). Biogeochemical
686 phosphorus cycling in groundwater ecosystems – Insights from South and Southeast Asian floodplain and
687 delta aquifers. *Science of the Total Environment*, 644, 1357–1370.
688 <https://doi.org/10.1016/j.scitotenv.2018.07.056>
- 689 Paytan, A., & McLaughlin, K. (2011). Tracing the Sources and Biogeochemical Cyclins in Aquatic Systems Using
690 Isotopes of Oxygen in Phosphate. In M. Baskaran (Ed.), *Handbook of Environmental Isotope Geochemistry: Vol*
691 *I* (pp. 419–436). Berlin, Heidelberg: Springer Berlin Heidelberg. [https://doi.org/10.1007/978-3-642-10637-](https://doi.org/10.1007/978-3-642-10637-8_21)
692 [8_21](https://doi.org/10.1007/978-3-642-10637-8_21)
- 693 Pistocchi, C., Tamburini, F., Gruau, G., Ferhi, A., Trevisan, D., & Dorioz, J. M. (2017). Tracing the sources and
694 cycling of phosphorus in river sediments using oxygen isotopes: Methodological adaptations and first
695 results from a case study in France. *Water Research*, 111, 346–356.
696 <https://doi.org/10.1016/j.watres.2016.12.038>
- 697 Quinton, J. N., Govers, G., Van Oost, K., & Bardgett, R. D. (2010). The impact of agricultural soil erosion on
698 biogeochemical cycling. *Nature Geoscience*, 3(5), 311–314. <https://doi.org/10.1038/ngeo838>
- 699 Senn, A. C., Kaegi, R., Hug, S. J., Hering, J. G., Mangold, S., & Voegelin, A. (2015). Composition and structure of
700 Fe(III)-precipitates formed by Fe(II) oxidation in water at near-neutral pH: Interdependent effects of
701 phosphate, silicate and Ca. *Geochimica et Cosmochimica Acta*, 162, 220–246.
702 <https://doi.org/10.1016/j.gca.2015.04.032>
- 703 Sharpley, A. N., Daniel, T., Sims, T., Lemunyon, J., Stevens, R., & Parry, R. (2003). *Agricultural Phosphorus and*
704 *Eutrophication Second Edition*. U.S. Department of Agriculture, Agricultural Research Service.
- 705 Shemesh, A., Kolodny, Y., & Luz, B. (1983). Oxygen isotope variations in phosphate of biogenic apatites, II.
706 Phosphorite rocks. *Earth and Planetary Science Letters*, 64, 398–404.
- 707 Shemesh, A., Kolodny, Y., & Luz, B. (1988). Isotope geochemistry of oxygen and carbon in phosphate and
708 carbonate of phosphorite francolite. *Geochimica et Cosmochimica Acta*, 52(11), 2565–2572.
709 [https://doi.org/10.1016/0016-7037\(88\)90027-0](https://doi.org/10.1016/0016-7037(88)90027-0)
- 710 Tamburini, F., Bernasconi, S. M., Angert, A., Weiner, T., & Frossard, E. (2010). A method for the analysis of the
711 $\delta^{18}\text{O}$ of inorganic phosphate extracted from soils with HCl. *European Journal of Soil Science*, 61(6), 1025–
712 1032. <https://doi.org/10.1111/j.1365-2389.2010.01290.x>
- 713 Tamburini, F., Pfahler, V., von Sperber, C., Frossard, E., & Bernasconi, S. M. (2014). Oxygen Isotopes for
714 Unraveling Phosphorus Transformations in the Soil–Plant System: A Review. *Soil Science Society of America*
715 *Journal*, 78(1), 38–46. <https://doi.org/10.2136/sssaj2013.05.0186dgs>
- 716 Thomson-Bulldis, A., & Karl, D. (1998). Application of a novel method for phosphorus determinations in the
717 oligotrophic North Pacific Ocean. *Limnology and Oceanography*, 43(7), 1565–1577.
718 <https://doi.org/10.4319/lo.1998.43.7.1565>
- 719 Vennemann, W. T., Fricke, C. H., Blake, R. E., O’Neil, J. R., & Colman, A. (2002). Oxygen isotope analysis of
720 phosphates: a comparison of techniques for analysis of Ag_3PO_4 . *Chemical Geology*, 185, 321–336.
721 [https://doi.org/10.1016/S0009-2541\(01\)00413-2](https://doi.org/10.1016/S0009-2541(01)00413-2)
- 722 Wetzel, R. G. (2001). The Phosphorus Cycle. In *Limnology: Lake and River Ecosystems* (3rd ed., pp. 242–250). San
723 Diego, California: Academic Press. [https://doi.org/10.1016/S0074-6142\(08\)62697-2](https://doi.org/10.1016/S0074-6142(08)62697-2)
- 724 Young, M. B., McLaughlin, K., Kendall, C., Stringfellow, W., Rollog, M., Elsbury, K. E., et al. (2009).
725 Characterizing the Oxygen Isotopic Composition of Phosphate Sources to Aquatic Ecosystems.
726 *Environmental Science & Technology*, 43(14), 5190–5196. Retrieved from
727 [http://10.0.3.253/es900337q%0Ahttps://search.ebscohost.com/login.aspx?direct=true&db=bsu&AN=43564](http://10.0.3.253/es900337q%0Ahttps://search.ebscohost.com/login.aspx?direct=true&db=bsu&AN=43564946&site=ehost-live)
728 [946&site=ehost-live](http://10.0.3.253/es900337q%0Ahttps://search.ebscohost.com/login.aspx?direct=true&db=bsu&AN=43564946&site=ehost-live)
- 729 Yuan, H., Li, Q., Kukkadapu, R. K., Liu, E., Yu, J., Fang, H., et al. (2019). Identifying sources and cycling of
730 phosphorus in the sediment of a shallow freshwater lake in China using phosphate oxygen isotopes.
731 *Science of The Total Environment*. <https://doi.org/10.1016/j.scitotenv.2019.04.322>
- 732 Zohar, I., Shaviv, A., Klass, T., Roberts, K., & Paytan, A. (2010). Method for the analysis of oxygen isotopic
733 composition of soil phosphate fractions. *Environmental Science and Technology*, 44(19), 7583–7588.
734 <https://doi.org/10.1021/es100707f>
- 735